Reflection coefficient of low-energy light ions

M. Vicanek and H. M. Urbassek
Institut für Theoretische Physik, P. O. Box 3329, W-3300 Braunschweig, Federal Republic of Germany
(Received 23 April 1990; revised manuscript received 19 June 1991)

We present a model for the slowing down and transport of light ions in the energy range between some tens of eV and some tens of keV in solids. The approach chosen here for low energies is based on the so-called age theory, and is augmented by the single-collision approximation for higher energies. These energy regimes are classified by the number of hard collision events ν experienced by the projectile before coming to rest. Technically, ν is defined as the ratio of the total range to the transport mean free path of the ion. In both the multiple- and the single-collision regimes, the particle reflection coefficient R_N is shown to be a universal function of ν and $\cos^2\theta_0$, where θ_0 denotes the bombarding angle. A simple-to-use expression for R_N is derived for the entire energy range by interpolation of the two limiting cases. Good agreement is found with a large number of experimental data.

I. INTRODUCTION

Reflection of light ions with energies in the eV to keV range from solid surfaces is of great importance for nuclear-fusion research where the interaction of plasma particles with the first wall constitutes one of the major problems. The subject has been investigated for decades, and a vast amount of data has been accumulated both from experiments and computer simulations.[1-5]

On the analytical side, the single-collision model for light-ion reflection was developed long ago, originally applied to protons in the middle-keV range.[6] Then, by allowing for screened cross sections, the model has been extended down to lower energies[7] and, by taking more accurate account of the electronic stopping,[8] also to higher energies. Driven by its success, the scheme has been extended still further to cover also heavier ions (or lighter targets) by making allowance for elastic energy loss,[9] and more recently, a generalization to non-normal incidence has been achieved.[10]

At lower bombarding energies, however, analytical theory has been somewhat cumbersome. The conventional approach consists in computing spatial moments of the ion distribution function and reconstructing the value at the surface from these.[11-13] Not only does this method have principal uncertainties with regard to the reconstruction, it also introduces an additional difficulty due to the assumption of an infinite medium. Here, the surface enters merely as a reference plane which, unlike reality, may be crossed by the projectile repeatedly. Since the associated error increases with increasing reflection, a subsequent correction has to be introduced in one way[14,12] or another.[13] Altogether, the method demands quite some labor, and the results are not obtained in an explicit form. Closed expressions for the reflection coefficient have been given only on empirical grounds.[4,5] In view of the elegant description by the single-collision model in the complementary regime, this situation must appear highly unsatisfactory.

This paper aims at filling the gap by presenting a simple model for the low-energy reflection coefficient of light ions. The method which we employ has been developed some time ago[15,16] and is known as *age theory* in neutron and electron transport calculations. In Sec. II we introduce this scheme in the context of light ion transport. Then, in Sec. III we apply the method to the calculation of the reflection coefficient. In Sec. IV we extend our model to cover higher energies by coupling it to the single-collision picture. Results and comparison to experiments are given in Sec. V, followed by a discussion in Sec. VI. The paper ends with an itemized conclusion.

II. LIGHT-ION TRANSPORT

Consider a light ion slowing down in a target consisting of randomly distributed atoms of number density N. Let $\Phi(\mathbf{r},E,\mathbf{\Omega})dE\,d^2\Omega$ be the time-integrated average ion flux at point $\mathbf{r}$ within the energy interval (E,dE) and solid angle $(\mathbf{\Omega},d^2\Omega)$. Then a forward transport equation for the ion flux is readily written down,[17]

$$\mathbf{\Omega}\cdot\nabla\Phi(r,E,\mathbf{\Omega})=N\int dE'd^2\Omega'[K(E',\mathbf{\Omega}'\rightarrow E,\mathbf{\Omega})\Phi(\mathbf{r},E',\mathbf{\Omega}')-K(E,\mathbf{\Omega}\rightarrow E',\mathbf{\Omega}')\Phi(\mathbf{r},E,\mathbf{\Omega})]$$
$$+N\frac{\partial}{\partial E}[S_e(E)\Phi(\mathbf{r},E,\mathbf{\Omega})]+Q(\mathbf{r},E,\mathbf{\Omega})\ . \tag{1}$$

Here, $Q(\mathbf{r},E,\mathbf{\Omega})$ denotes a source of ions and $K(E,\mathbf{\Omega}\rightarrow E',\mathbf{\Omega}')dE'd^2\Omega'$ is the elastic cross section for the ion moving at energy E in the direction $\mathbf{\Omega}$ to scatter at a resting target atom into energy E' and direction $\mathbf{\Omega}'$. Owing to energy and momentum conservation, it is

$$K(E,\mathbf{\Omega}\rightarrow E',\mathbf{\Omega}')dE'd^2\Omega'=\sigma(E,T)dT\,\delta(\mathbf{\Omega}\cdot\mathbf{\Omega}'-\hat{\mu})\frac{d^2\Omega}{2\pi}\ , \tag{2}$$

where $T=E-E'$ is the transferred energy and $\hat{\mu}$ is the cosine of the scattering angle in the laboratory system, given by kinematics, Eq. (A2). $\sigma(E,T)dT$ is the cross section for energy transfer in the usual notation.[18] Finally, in Eq. (1) $S_e(E)$ is the electronic stopping cross section.

Since we are interested in a planar geometry, the number of independent variables can be reduced. Let z denote the depth in the target measured from the surface and μ the direction cosine with respect to the inward surface normal. Then the flux can be integrated over the two remaining space coordinates x and y as well as the azimuth angle ϕ to yield

$$\Phi(z,E,\mu)=\int_{-\infty}^{\infty}\int_{-\infty}^{\infty}dx\,dy\int_0^{2\pi}d\phi\,\Phi(\mathbf{r},E,\Omega)\ . \tag{3}$$

$\Phi(z,E,\mu)$ is the mean number of ions passing through a plane at z with energy (E,dE) within a cone $(\mu,d\mu)$. Multiplying Eq. (1) by a Legendre polynomial $P_l(\mu)$ and integrating over μ, we obtain a set of integro-differential equations:

$$(2l+1)^{-1}\frac{\partial}{\partial z}[(l+1)\Phi_{l+1}(z,E)+l\Phi_{l-1}(z,E)]$$
$$=N\int dT[P_l(\hat{\mu})\sigma(E+T,T)\Phi_l(z,E+T)-\sigma(E,T)\Phi_l(z,E)]+N\frac{\partial}{\partial E}[S_e(E)\Phi_l(z,E)]+Q_l(z,E)\ . \tag{4}$$

Here, $\Phi_l(z,E)$ denote the Legendre moments of the flux:

$$\Phi_l(z,E)=\tfrac{1}{2}\int_{-1}^{1}d\mu\,P_l(\mu)\Phi(z,E,\mu)\ . \tag{5}$$

Now we perform the approximations which constitute the age theory. For $l=0$, Eq. (4) involves the two Legendre moments Φ_0 and Φ_1. For $l=1$, it contains Φ_0, Φ_1, and Φ_2. Neglecting Φ_2 compared to Φ_0, however, results in a closed system of two equations for Φ_0 and Φ_1 only. Furthermore, we expand the integrand in Eq. (4) in a Taylor series:

$$\sigma(E+T,T)\Phi_l(z,E+T)=\sigma(E,T)\Phi_l(z,E)+T\frac{\partial}{\partial E}\sigma(E,T)\Phi_l(z,E)+\cdots\ . \tag{6}$$

We take into account two terms for $l=0$ and one term for $l=1$ as they give the first nonvanishing approximations of the scattering integral in Eq. (4). Thus we arrive at the set of equations

$$\begin{aligned}&\frac{\partial}{\partial z}\Phi_1(z,E)=N\frac{\partial}{\partial E}S(E)\Phi_0(z,E)+Q_0(z,E)\ ,\\ &\frac{1}{3}\frac{\partial}{\partial z}\Phi_0(z,E)=-N\sigma_{\rm tr}(E)\Phi_1(z,E)+Q_1(z,E)\ ,\end{aligned} \tag{7}$$

with the total stopping cross section $S(E)$,

$$\begin{aligned}&S(E)=S_n(E)+S_e(E)\ ,\\ &S_n(E)=\int T\sigma(E,T)dT\ ,\end{aligned} \tag{8}$$

and the transport cross section $\sigma_{\rm tr}(E)$,

$$\sigma_{\rm tr}(E)=\int(1-\hat{\mu})\sigma(E,T)dT\ . \tag{9}$$

The two quantities $S(E)$ and $\sigma_{\rm tr}(E)$ represent the two basic aspects of slowing down, namely, *stopping* and *deflection*. Higher-order approximations would also contain energy loss straggling, higher angular moments of the cross section, and correlations between energy loss and scattering angle.

It may be helpful to note that for light ion scattering, the nuclear stopping cross section and the transport cross section are related by kinematics. In fact, making use of Eq. (A2), it is

$$\sigma_{\rm tr}(E)\simeq\frac{M_2}{2M_1E}S_n(E)\ , \tag{10}$$

where M_1 and M_2 denote the projectile and target mass, respectively.

We cast Eq. (7) in a convenient nondimensional form by introducing the independent variables

$$x=N\sigma_{\rm tr}(E_0)z \tag{11}$$

and

$$t=\tfrac{1}{3}\sigma_{\rm tr}(E_0)^2\int_E^{E_0}\frac{dE'}{S(E')\sigma_{\rm tr}(E')}\ . \tag{12}$$

Here x is the depth measured in units of the transport mean free path $\lambda_{\rm tr}$ at the bombarding energy E_0,

$$\lambda_{\rm tr}(E_0)=[N\sigma_{\rm tr}(E_0)]^{-1}\ , \tag{13}$$

while t takes on the meaning of a symbolic time, the so-called *Fermi age*. From Eq. (12) one observes that as the ion loses energy, the corresponding age increases. It is important to note that there is an upper limit t_0 for the age

$$t_0=\tfrac{1}{3}\sigma_{\rm tr}(E_0)^2\int_0^{E_0}\frac{dE}{S(E)\sigma_{\rm tr}(E)}\ . \tag{14}$$

For Φ_0 and Φ_1 we also introduce new variables, the *slowing down density* $\chi(x,t)$,

$$\chi(x,t)dx=2NS(E)\Phi_0(z,E)dz \tag{15}$$

and the *particle current* $j(x,t)$,

$$j(x,t)dt=2\Phi_1(z,E)dE\ . \tag{16}$$

With this we obtain from Eq. (7), neglecting the sources for the moment,

$$\begin{aligned}&\frac{\partial}{\partial t}\chi(x,t)+\frac{\partial}{\partial x}j(x,t)=0\ ,\\ &j(x,t)=-\frac{\partial}{\partial x}\chi(x,t)\ .\end{aligned} \tag{17}$$

Equations (17) have the familiar form of ordinary diffusion equations. They constitute the well-known age theory.

III. REFLECTION OF LIGHT IONS

In the following we specify the sources and boundary conditions for light ion bombardment of a target surface. With regard to the source, we face the problem of properly incorporating the bombarding angle into a P_1 approximation scheme.[17] In order to overcome this difficulty we split up the particle flux into two parts:

$$\Phi(z,E,\mu)=\Phi^b(z,E,\mu)+\Phi^a(z,E,\mu) , \tag{18}$$

where Φ^b describes the particle motion *before* its first violent collision and Φ^a corresponds to the particle motion *after* the first violent collision. Consequently, Φ^b will be strongly peaked in the direction of the incident beam whereas Φ^a will be more or less isotropic. One may then expect that Φ^a should be described quite well by the diffusion equation (7). What remains is to derive an expression for Φ^b and the corresponding coupling to Φ^a.

Let the bombarding particle impinge on the target surface with energy E_0 and polar angle $\theta_0=\arccos\mu_0$. If σ_{tr} is viewed as the cross section for wide-angle collisions, then the probability for the particle to undergo such a collision within a layer of thickness dz is $N\sigma_{tr}(E_0)dz/\mu_0$. Thus the first part of the flux Φ^b may be written as

$$\Phi^b(z,E,\mu)=\mu_0^{-1}\exp[-N\sigma_{tr}(E_0)z/\mu_0] \times\delta(E-E_0)\delta(\mu-\mu_0) . \tag{19}$$

Here we have neglected the effect of soft collisions and electronic stopping as a first approximation. A higher approximation would have to incorporate slowing down and angular spreading.

From particle conservation we find for the source in Eq. (7)

$$Q_0(z,E,\mu)=\frac{N\sigma_{tr}(E_0)}{2\mu_0} \times\exp[-N\sigma_{tr}(E_0)z/\mu_0]\delta(E-E_0) . \tag{20}$$

The anisotropic part of the source, Q_1 in Eq. (7), is set equal to zero. This corresponds to the fact that the primary flux Φ^b decays with λ_{tr} as the characteristic length which is the average distance needed for complete randomization of the direction of motion.

The source Eq. (20) in Eq. (7) is equivalent to the initial condition

$$\chi(x,t=0)=\mu_0^{-1}e^{-x/\mu_0} \tag{21}$$

for Eq. (17).

The present scheme has to be completed by a semi-infinite medium boundary condition. In the diffusion formalism the target surface acts like a perfectly absorbing wall, thus we require that the slowing down density vanishes at the surface:

$$\chi(x=0,t)=0 . \tag{22}$$

Equations (17), (21), and (22) entirely describe the reflection within the present scheme.

In the following we present a solution to this reflection problem. In principle, a solution for the slowing down density χ and the particle current j may be obtained for the entire target volume. Here, however, we are interested in surface quantities primarily. Thus we use a method which allows direct evaluation of the surface quantities and avoids the extra labor of calculating the whole spatial dependence.

Introducing the Laplace transform of the slowing down density

$$\tilde{\chi}(x,p)=\int_0^\infty dt\, e^{-pt}\chi(x,t) , \tag{23}$$

and correspondingly for the particle current $\tilde{j}(x,p)$, the diffusion equations (17) become

$$\begin{aligned} &p\tilde{\chi}(x,p)+\frac{\partial}{\partial x}\tilde{j}(x,p)=\mu_0^{-1}e^{-x/\mu_0} , \\ &\tilde{j}(x,p)=-\frac{\partial}{\partial x}\tilde{\chi}(x,p) . \end{aligned} \tag{24}$$

Here we have incorporated the initial condition (21) already. The straightforward solution of Eq. (24) is

$$\begin{aligned} &\tilde{\chi}(x,p)=C(p)e^{-\sqrt{p}x}+\frac{\mu_0^{-1}}{p-\mu_0^{-2}}e^{-x/\mu_0} , \\ &\tilde{j}(x,p)=\sqrt{p}\ C(p)e^{-\sqrt{p}x}+\frac{\mu_0^{-2}}{p-\mu_0^{-2}}e^{-x/\mu_0} , \end{aligned} \tag{25}$$

where $C(p)$ is a function determined by the boundary condition (22).

Consider the solution, Eq. (25), at the surface $x=0$. Then the unknown function $C(p)$ may be eliminated, yielding

$$\tilde{\chi}(x=0,p)=\frac{1}{\sqrt{p}}\tilde{j}(x=0,p)+\frac{\mu_0^{-1}}{\sqrt{p}\,(\sqrt{p}+\mu_0^{-1})} . \tag{26}$$

In the following we consider all quantities at the surface $x=0$ only, thus we drop the space variable x in the list of arguments. Taking account of the boundary condition, Eq. (22), it follows

$$\tilde{j}(p)=-\frac{\mu_0^{-1}}{\sqrt{p}+\mu_0^{-1}} , \tag{27}$$

which may be readily inverted to direct space[19] to give

$$j(t)=-\mu_0^{-1}\left[\frac{1}{\sqrt{\pi t}}-\mu_0^{-1}E(\sqrt{t}/\mu_0)\right] . \tag{28}$$

Here we used the abbreviation

$$E(z)=e^{z^2}\mathrm{erfc}z , \tag{29}$$

where erfcz denotes the complementary error function.[20] The total backscattering coefficient R_N is easily obtained. Noting that

$$R_N=-\int_0^{t_0}j(t)dt , \tag{30}$$

we get from Eq. (28) the simple result

$$R_N = 1 - E(\sqrt{t_0}/\mu_0) \ . \tag{31}$$

IV. EXTENSION TO HIGHER BOMBARDING ENERGIES

The essential quantity characterizing the transport within the present approach is the nondimensional parameter t_0 defined in Eq. (14). To examine the physical meaning of this number more closely, consider the simple case where scattering and stopping exhibit a power-law dependence on energy, with respective power exponents m and m_1. Thus it is $\sigma_{tr}(E) = (E/E_0)^{-2m}\sigma_{tr}(E_0)$ and $S(E) = (E/E_0)^{1-2m_1}S(E_0)$, and Eq. (14) yields

$$t_0 = \frac{E_0 \sigma_{tr}(E_0)}{6(m+m_1)S(E_0)} \ . \tag{32}$$

On the other hand, the mean range $R(E_0)$ of the ion is, in the continuous-slowing-down approximation,[21]

$$R(E_0) = \int_0^{E_0} \frac{dE}{NS(E)} = \frac{E_0}{2m_1 NS(E_0)} \ . \tag{33}$$

Combining Eqs. (32) and (33) we obtain

$$t_0 = \frac{1}{3(1+m/m_1)} \frac{R(E_0)}{\lambda_{tr}(E_0)} \ , \tag{34}$$

i.e., t_0 is proportional to the ratio ν of the mean range and the transport mean free path,

$$\nu = R/\lambda_{tr} \ . \tag{35}$$

The quantity ν has an intuitive meaning: it is the mean number of wide-angle collisions suffered by the ion before slowing down to rest.

For the energy range under consideration—some tens of eV to some tens of keV—scattering is roughly governed by $m \simeq \frac{1}{2}$, and stopping is velocity proportional, i.e., $m_1 = \frac{1}{4}$. Thus Eq. (34) becomes

$$t_0 \simeq \tfrac{1}{9}\nu \ . \tag{36}$$

Examination of Eq. (31) for the limiting case $t_0 \gg 1$ shows with the aid of Eq. (36) that the reflection coefficient behaves like

$$R_N \sim 1 - \frac{3\mu_0}{\sqrt{\pi\nu}} + \frac{27}{2\sqrt{\pi}} \frac{\mu_0^3}{\nu^{3/2}} \ , \quad \nu \gg 1 \ . \tag{37}$$

The square root of ν in the second term in this expression reflects the random-walk diffusionlike nature of the transport in this case.

In the opposite limit $t_0 \ll 1$, Eq. (31) does not give a reasonable result since the assumptions underlying age theory are violated. For this case we use the single-collision model known from literature.[10] However, for our purpose we wish to express the reflection coefficient in terms of the quantity ν, thus we present a derivation in the Appendix. The result is

$$R_N \simeq (\tfrac{3}{2} - \sqrt{2})\nu/\mu_0^2 \ , \quad \nu \ll 1 \ . \tag{38}$$

One may interpolate the two limits (37) and (38) by the expression

$$R_N = \left[1 + a_1 \frac{\mu_0}{\sqrt{\nu}} + a_2 \frac{\mu_0^2}{\nu} + a_3 \frac{\mu_0^3}{\nu^{3/2}} + a_4 \frac{\mu_0^4}{\nu^2} \right]^{-1/2} , \tag{39}$$

with

$$\begin{aligned} a_1 &= \frac{6}{\sqrt{\pi}} \simeq 3.39 \ , \quad a_2 = \frac{27}{\pi} \simeq 8.59 \ , \\ a_3 &= \frac{27}{\sqrt{\pi}} \left[\frac{4}{\pi} - 1 \right] \simeq 4.16 \ , \\ a_4 &= \left[\tfrac{3}{2} - \sqrt{2} \right]^{-2} \simeq 135.9 \ . \end{aligned} \tag{40}$$

Equation (39) is our central result.

V. RESULTS

To evaluate Eq. (39) for a specific case, the range R and the transport mean free path λ_{tr} have to be computed. We used the Kr-C potential[22] for elastic interaction and the LSS expression for electronic stopping.[23] Figure 1 depicts the two contributions for the stopping of hydrogen in nickel. Clearly, stopping is dominated by electronic interaction in the entire energy regime shown.

Figure 2 shows the transport mean free path λ_{tr} and the ion range R for the same system. The range has been obtained by direct numerical integration of Eq. (33), and λ_{tr} by Eq. (10). One observes that for energies below around 10 keV, the transport mean free path is smaller than the range, which means $\nu > 1$. Above 10 keV, it is $\nu < 1$.

Figure 3 shows the reflection coefficient at normal incidence. The solid line represents our analytical formula, Eq. (39). In order to check the various approximations entering the derivation of the analytical expression, we

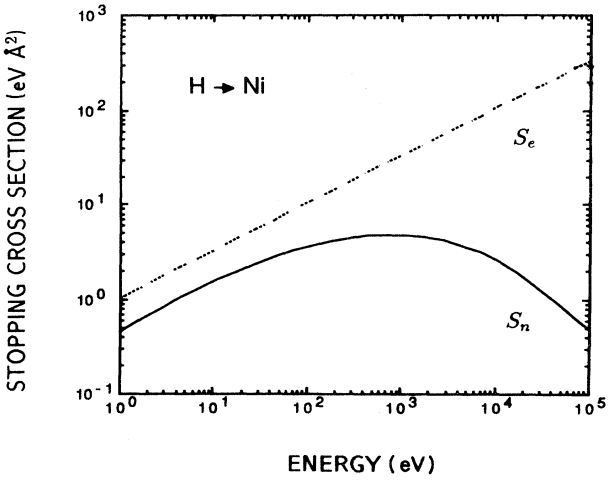

FIG. 1. Nuclear and electronic stopping cross section for hydrogen in nickel.

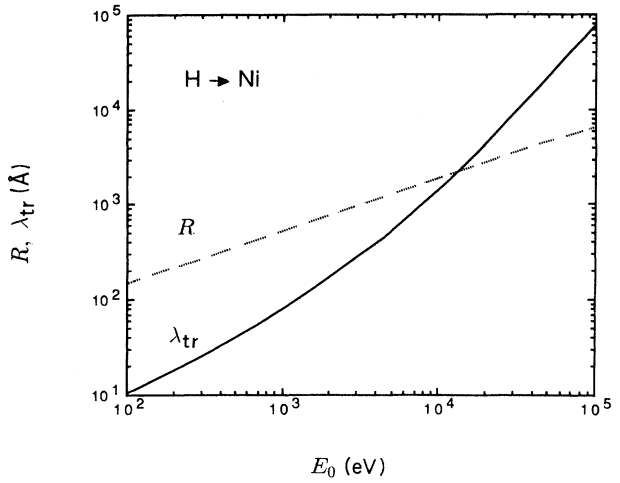

FIG. 2. Total range R and transport mean free path λ_{tr} for hydrogen in nickel.

have performed a large number of simulations of H, D, and He reflection from various targets for a wide range of incident energies. These calculations were performed with a Monte Carlo code[24] which is designed to solve Eq. (1). The same physical input, i.e., Kr-C potential and LSS electronic stopping, have been used for both the simulation and the analytical model. Excellent scaling is observed: the simulated data points in Fig. 3 lie on a single curve when plotted as a function of ν. This curve coincides rather well with the solid line in Fig. 3, Eq. (39). We thus conclude that the present theory provides a simple and accurate solution of Eq. (1) for the reflection coefficient.

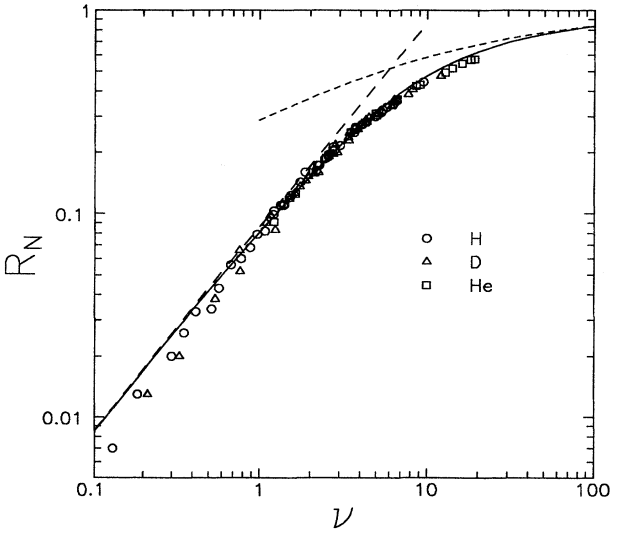

FIG. 3. Reflection coefficient for normal incidence. The inset specifies the projectile type. The target elements and the range of energies covered correspond to those in Fig. 4. Data points: simulation results. Solid drawn line: analytical theory Eq. (39). Long-dashed line: single-collision approximation (38). Short-dashed line: age approximation, Eq. (31) with (36).

We furthermore include in Fig. 3 the single-collision approximation (38) (long-dashed line) and the age result (31) (short-dashed line). We see that the single-collision result describes the reflection process well up to $\nu \lesssim 2$. The proper regime of validity of the age theory starts only at $\nu \gtrsim 20$, which is hardly ever reached in experiments. It is obvious that without a knowledge of the behavior of the reflection coefficient for large ν, an interpolation formula for the experimentally interesting regime $2 < \nu < 20$ could not have been designed.

Figures 4(a)–4(c) show the calculated reflection coefficient of H, D, and He ions at normal incidence as a function of ν in comparison to measured values for a wide range of target materials. The experimental data are taken from compilations by Tabata *et al.*[3] and by Eckstein and Verbeek in Ref. 5, covering an energy range of 50 eV $\leq E_0 \leq$ 50 keV, or, in dimensionless units,[18] $5\times10^{-3} \leq \epsilon \leq 25$. Obviously, the scaling of the data as well as their agreement with the theoretical prediction is worse than for the simulation, Fig. 3. Certainly, one has to bear in mind that the measurements were performed by different groups, and the scatter is up to a factor of 2 even within the data of a single group. This, however, could explain at most the spread of the data but not the systematic deviations. In particular, the measured reflection coefficient is significantly below the theoretical value for certain projectile-target combinations. We wish to mention three effects which may contribute to the systematic overestimation of our theory.

(i) An underestimation of the electronic stopping by the LSS expression: A higher electronic stopping would result in a smaller total range thus shifting the data points in Figs. 4(a)–4(c) to the left, giving better agreement with the theory.

(ii) Lattice effects: The experiments underlying Fig. 4 have been performed under high-fluence conditions on polycrystalline targets. Channeling in the microcrystallites and texture effects can reduce the overall reflection coefficient in comparison to a truly random target.

(iii) Target oxidation: Several of the target materials that show discrepancies between experiment and theory are good candidates for contamination with oxygen. This would reduce the reflection coefficient. Implantation of the bombarding gas will have the same effect.

Measurements of the reflection coefficient for oblique incidence are comparatively scarce. Figure 5 shows data for ^{3}He bombardment of Ni, taken from Ref. 25. It is seen that the Monte Carlo results fall well on one line, supporting the idea that ν/μ_0^2 is an adequate scaling parameter for our problem. These Monte Carlo results are excellently reproduced by our analytical theory, Eq. (39), for $\nu/\mu_0^2 \lesssim 10$. For more glancing incidence, theory overestimates the Monte Carlo results. This failure can be attributed to age theory which predicts a reflection coefficient of unity for $\nu/\mu_0^2 \to \infty$, cf. Eq. (37), whereas in the full transport equation, and in the Monte Carlo solution, there exists a finite probability for the projectile to be implanted in the target even in this case. Finally we observe that the agreement of the experimental data with

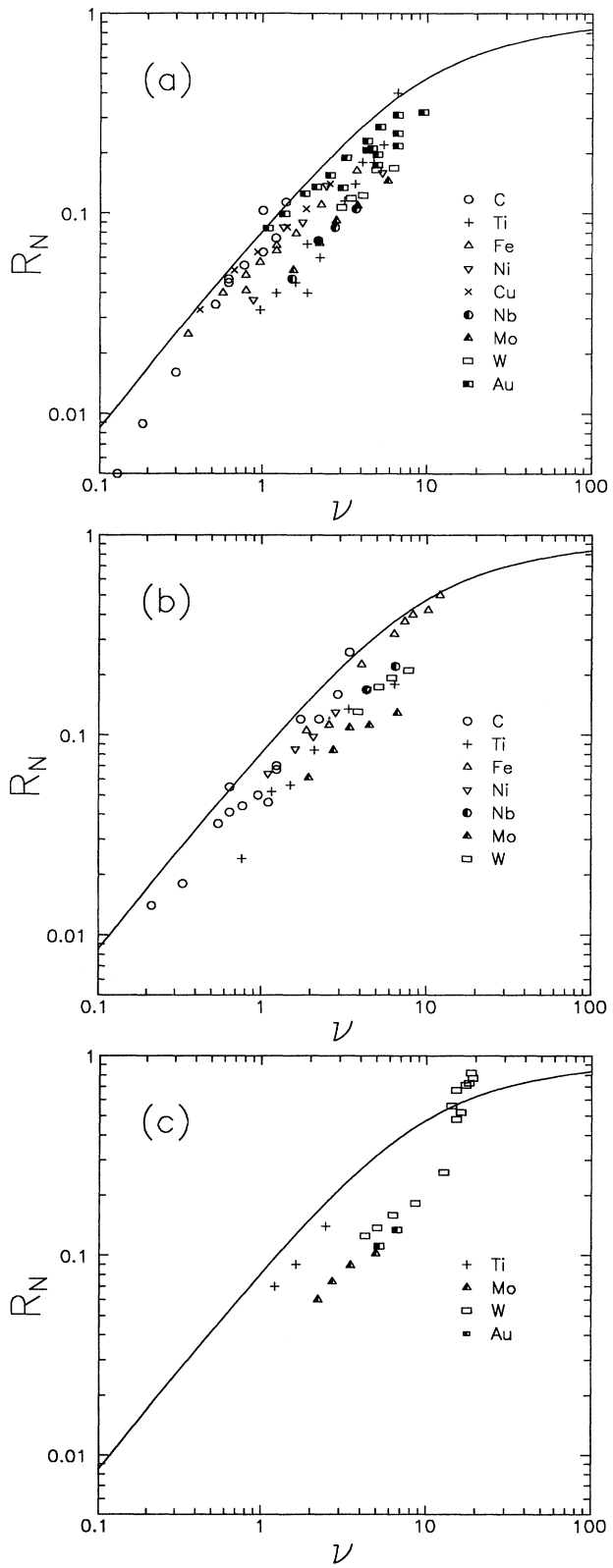

FIG. 4. Reflection coefficient of light ions for normal incidence. Symbols represent experimental data, the solid drawn line is Eq. (39). The inset in each figure specifies the target material. (a) Proton bombardment. (b) Deuterium bombardment. (c) Helium bombardment.

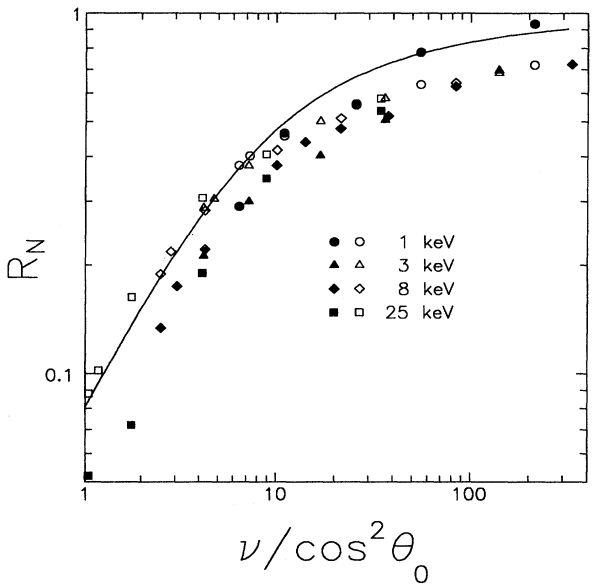

FIG. 5. Reflection coefficient of ^{3}He from Ni as a function of the scaling parameter $\nu/\cos^2\theta_0$. The solid symbols represent experimental data, the empty symbols show simulation results, the solid drawn line is Eq. (39). The inset specifies the bombarding energy.

the Monte Carlo results is very satisfactory over all the range of μ_0 depicted in Fig. 5, with the exception of the case of 1 keV bombardment. In this case the projectiles have a high chance of being reflected directly from the outermost surface layer; since they do not penetrate into the target, transport theory as described by Eq. (1) does not apply.

In Fig. 6 we present the energy spectrum of low-energy deuterium reflected from nickel. The dashed line has been obtained from Eq. (28) using the appropriate transformation $j(t)dt = j(E)dE$. It is seen that the age theory overestimates the simulated spectrum at energies close to the bombarding energy and underestimates it at lower energies. This finding is explained by the fact that within

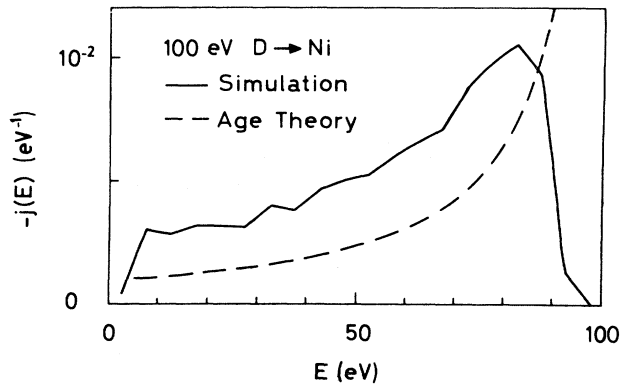

FIG. 6. Spectrum of low-energy deuterium reflected from a nickel surface at normal incidence.

the framework of the age theory, any correlation between scattering and energy loss in a single elastic collision is disregarded. Hence, in this picture, the projectile may be reflected by a head-on collision without energy loss. This gives rise to a (slight) divergence of the spectrum at the bombarding energy. In the simulation, of course, energy loss and scattering in a single collision are properly treated; hence no divergence occurs. However, a pronounced peak at around 80 eV is left.

VI. DISCUSSION

A theoretical description of the transport and reflection of light ions in the low-energy regime is difficult for the following reasons.

(i) Two forces of different nature but comparable magnitude act on the projectile: nuclear and electronic interaction with the target. While nuclear interaction is entirely responsible for *scattering,* electronic interaction constitutes the major contribution to *stopping.* The energy dependence of these two forces is quite different (see Fig. 1), thus their relative importance varies substantially with bombarding energy.

(ii) The competition of scattering and stopping is quantified by the ratio ν of the range and the transport mean free path. The two possible extremes $\nu \gg 1$ and $\nu \ll 1$ result in a diffusionlike behavior and a straight-line motion, respectively. The transport of low-energy light ions is just in between these two limiting cases.

(iii) Since the reflection coefficient of light ions may be quite high, one needs to incorporate the influence of the surface.

In view of these difficulties, a transport theory that attempts to provide a closed-form solution clearly needs to introduce simplifications at some point. The two essential approximations underlying age theory are the neglect of Φ_2 as against Φ_0 in Eq. (4) and the truncation of the Taylor series in Eq. (6). The former leads to a closed system of coupled equations for Φ_0 and Φ_1, which is known as the P_1 approximation.[26] The latter results in an approximation of the scattering integral operator by a differential operator and is known as continuous slowing down.

It is worthwhile to note that the conventional derivation of the P_1 approximation[26] is based on an expansion of the flux into a Legendre series:

$$\Phi(\mu)=\sum_{l=0}^{\infty}(2l+1)\Phi_l P_l(\mu)\ , \tag{41}$$

which is truncated for $l>1$. This procedure is unnecessarily restrictive since it is sufficient to merely require $\Phi_2 \ll \Phi_0$. Take, for example, a surface from which particles escape according to the Knudsen cosine law. In the present notation, this corresponds to a flux $\Phi(\mu)=$const. for $\mu<0$ and $\Phi(\mu)=0$ for $\mu>0$. Clearly, the condition $\Phi_2 \ll \Phi_0$ is satisfied as Φ_2 vanishes altogether, cf. Eq. (5). However, a representation of the flux by truncating the series in Eq. (41), $\Phi(\mu)=\text{const}\times(1/2+3\mu/4)$, would be rather poor. This illustrates that the first two Legendre moments Φ_0 and Φ_1 may be calculated with reasonable accuracy within the P_1 approximation even in cases where the angular flux is not a linear function of the direction cosine μ. Conversely, the P_1 approximation provides only little information on the angular distribution.

The condition $\Phi_2 \ll \Phi_0$ is clearly violated before the projectile suffers its first hard collision. The collimated part of the flux has been split off and treated separately (see Sec. III), although only in a somewhat intuitive way.

The continuous slowing down approximation, i.e., the truncation of the Taylor series, Eq. (6), holds for $\gamma E \partial(\sigma\Phi)/\partial E \ll \sigma\Phi$, where γE is the maximum kinematic energy transfer. As it is $\gamma=4M_1M_2/(M_1+M_2)^2 \ll 1$ for very different masses, the above condition essentially requires that the flux be a well-behaved function of energy. This is uncritical except near the bombarding energy.

The validity of the approximations entering the present theory is demonstrated by good agreement with the numerical solution of the transport equation with the help of computer simulation, where the same physical input has been used. Here, a large number of target materials and a wide range of energies have been covered, showing excellent scaling as predicted by the present scheme.

Limitations of the model become apparent in calculations of the energy spectrum of reflected particles. Here, age theory is found to be too restrictive by neglecting the correlation between scattering and energy loss in an elastic collision.

Our final result, Eq. (39), is expressed in terms of the ratio ν of the mean ion range R and the transport mean free path λ_{tr}. This ratio has the intuitive interpretation of the number of wide-angle collisions of the ion during slowing down. The representation of the backscattering coefficient as a function of ν gives a universal function for all projectile and target combinations. A similar scaling has been used previously[27] in the diffusion regime, $\nu \gg 1$. Our theory is more general in the regime of energies covered, and gives explicit results.

For empirical fits, the reflection coefficient has often been plotted as a function of the nondimensional energy ε.[5,28] From a theoretical point of view, this is not adequate since the reflection coefficient should be a different function of ε for each projectile. In practice, however, this difference turns out to be small because two effects nearly compensate: Heavier projectiles suffer less electronic stopping, while at the same time they get less deflected in elastic collisions. Consequently, it happens that both the range and the transport mean free path are larger than for lighter projectiles, leaving the ratio ν about constant.

The reflection coefficient increases monotonously for increasing bombarding angle, approaching unity at grazing incidence. This behavior is also found in experiments. It is a curious fact that according to formula (39), the reflection coefficient depends on the incidence angle and energy only through the combined expression μ_0^2/ν. This does not appear to have an immediate physical meaning.

The range of applicability of the present model has, of course, limitations with regard to both incidence angle

and energy. On the low-energy side, say below 10 eV, the binary collision assumption inherent in the Boltzmann equation (1) breaks down. Perhaps even more important are attractive forces between the ion and the surface which may have a decisive influence on the reflection coefficient.

For high energies, about $\varepsilon > 10$, another difficulty appears: Even though the single-collision picture should be an excellent description, it is not applicable in the way presented here. For such energies, scattering is governed by weakly screened Coulomb interaction, thus the cross section is very strongly forward peaked. As a result, the transport mean free path λ_{tr} [Eqs. (13) and (9)] is mainly determined by *forward* scattering. On the other hand, the reflection coefficient is evidently determined by *backward* scattering. Consequently, a representation of the reflection coefficient in terms of λ_{tr}, or more precisely ν, is no longer appropriate. In fact, the constant a_2 in Eq. (39) becomes energy dependent.

The theory is not expected to give a correct description for grazing incidence. In this case, the first collision with a surface atom leads to scattering preferably *away* from the target because of broken azimuthal symmetry of possible impact parameters. This effect is not included in the Boltzmann equation nor in the single collision model. A very rough estimate based on a simple geometrical argument—borrowed from the theory of shadow cones—shows that the corresponding critical incidence angle θ_0 is given by $\cos\theta_0 \simeq b/a$, where a is the interatomic spacing and b is determined as the separation at which the ion-target potential $V(r)$ is equal to the bombarding energy, $V(b)=E_0$. Moreover, the details of the surface structure certainly cannot be disregarded for glancing angles. The fact that Eq. (39) still seems to yield reasonable results even for grazing bombardment may be a lucky coincidence.

The main advantage of the present theory over other analytical treatments lies in its simplicity and transparency. All beam and target parameters are condensed to one dimensionless number ν, and the reflection coefficient is expressed as a universal function of this number. Thus, the effect of different bombarding conditions is seen immediately. Likewise, the influence of the physical input is given explicitly.

VII. CONCLUSIONS

1. We have presented an analytical theory for the reflection of light ions at energies ranging from a few tens of eV to a few tens of keV.

2. The model is based on the so-called *age theory,* known from electron and neutron transport. This scheme provides a very simple description and is valid in the lower portion of energies considered here.

3. To extend the range of application we use the single-collision model for the higher energies. The two different schemes are connected via a simple interpolation.

4. Our central result, Eq. (39), is a simple formula for the reflection coefficient which contains the dependence on incidence angle and energy.

5. The energy dependence enters through the ratio ν of the mean ion range R and the transport mean free path λ_{tr} at the bombarding energy. The parameter ν has the intuitive meaning of the average number of wide-angle collisions for the projectile before slowing down to rest.

6. The reflection coefficient (39) has been found to be in good agreement with a large number of simulation data using the same physical input. This validates the analytical solution of the transport equation and verifies the approximations entering the calculation.

7. Measured reflection coefficients are well described by our theory for some projectile-target combinations and are overestimated for others. We ascribe the deviations to an underestimation of the electronic stopping by the LSS formula, and possibly also to target texture and contamination.

ACKNOWLEDGMENTS

We are grateful to Peter Sigmund for valuable comments. Financial support by the Deutsche Forschungsgemeinschaft is acknowledged.

APPENDIX

Here we derive the reflection coefficient in the single-collision approximation, formula (38). The calculation is performed similarly to that of Ref. 10, the notation being somewhat different, though.

Let a light ion impinge on the target surface with energy E_0 at normal incidence. Suppose that it penetrates into the target along a straight trajectory to a depth z, where it undergoes a wide-angle collision, followed by another straight trajectory toward the surface (Fig. 7). Then the probability for the particle to leave the target is obtained by integration over all possible events:

$$R_N = N\int_0^\infty dz \int_{-1}^{0} d\hat{\mu}\,\sigma(E,\hat{\mu})\Theta(R - z - z/|\hat{\mu}|)\ . \tag{A1}$$

Here, $\sigma(E,\hat{\mu})d\hat{\mu}$ is the cross section for the projectile at energy E to scatter into the cone $(\hat{\mu},d\hat{\mu})$, where $\hat{\mu}$ is the cosine of the scattering angle:

$$\hat{\mu} = (1-T/E)^{-1/2}\left[1-\frac{M_1+M_2}{2M_1}\frac{T}{E}\right] \simeq 1-\frac{M_2}{2M_1}\frac{T}{E}\ . \tag{A2}$$

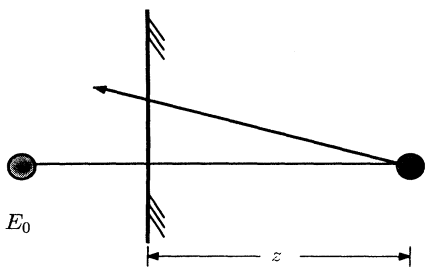

FIG. 7. Geometry of the single-collision model.

The approximation in Eq. (A2) is valid if the projectile mass M_1 is much smaller than the target mass M_2 since in that case, only a little amount of energy is transferred in a collision, $T \ll E$. Power cross sections in the usual notation[18]

$$\sigma(E,T)dT = C_m E^{-m} T^{-1-m} dT \tag{A3}$$

may be transformed through Eq. (A2) to

$$\sigma(E,\hat{\mu})d\hat{\mu} = \frac{1-m}{2^{1-m}} \sigma_{\rm tr}(E_0) \left[\frac{E}{E_0} \right]^{-2m} \frac{d\hat{\mu}}{(1-\hat{\mu})^{1+m}} . \tag{A4}$$

The Heaviside step function $\Theta(x)$ in Eq. (A1) ensures that the projectile may leave the target only if its total traveled path length is smaller than the mean range R.

The energy of the projectile at the collision E is smaller than the bombarding energy E_0 due to stopping,

$$\frac{dE}{dz} = -NS(E) . \tag{A5}$$

For powerlike stopping, $S(E) = S(E_0)(E/E_0)^{1-2m_1}$, integration of Eq. (A5) gives

$$E = (1 - z/R)^{1/2m_1} E_0 , \tag{A6}$$

where the total range R is given by Eq. (33). Inserting Eqs. (A4) and (A6) into Eq. (A1) we obtain

$$R_N = a \frac{R}{\lambda_{\rm tr}} \tag{A7}$$

with the numerical constant

$$a = \frac{1-m}{2^{1-m}} \int_{-1}^{0} \frac{d\hat{\mu}}{(1-\hat{\mu})^{1+m}} \int_{0}^{|\hat{\mu}|/(1+|\hat{\mu}|)} \frac{d\zeta}{(1-\zeta)^{m/m_1}} . \tag{A8}$$

It shows that a is not strongly dependent on the values of m and m_1 except when m approaches unity. For $m = \frac{1}{2}$ and $m_1 = \frac{1}{4}$, it is

$$a = \tfrac{3}{2} - \sqrt{2} . \tag{A9}$$

Vukanić *et al.*[10] give the approximate angular dependence of the reflection coefficient for the same case as

$$R_N(E_0,\mu_0) = R_N(E_0,\mu_0 = 1)/\mu_0^2 , \tag{A10}$$

valid except for glancing incidence.

[1] E. S. Mashkova and V. A. Molchanov, *Medium-Energy Ion Reflection from Solids* (North-Holland, Amsterdam, 1985).
[2] E. S. Mashkova, Radiat. Eff. **54**, 1 (1981).
[3] T. Tabata, R. Ito, Y. Itikawa, N. Itoh, and K. Morita, At. Data Nucl. Data Tables **28**, 493 (1983).
[4] T. Tabata, R. Ito, Y. Itikawa, N. Itoh, K. Morita, and H. Tawara, (unpublished).
[5] R. A. Langley, J. Bohdansky, W. Eckstein, P. Mioduszewski, J. Roth, E. Taglauer, E. W. Thomas, H. Verbeek, and K. L. Wilson, Nuclear Fusion (1984) (special issue).
[6] G. M. McCracken and N. J. Freeman, J. Phys. B **2**, 661 (1969).
[7] J. Vukanić and P. Sigmund, Appl. Phys. **11**, 265 (1976).
[8] W. Eckstein and J. P. Biersack, Z. Phys. A **310**, 1 (1983).
[9] R. Wedell, Appl. Phys. A **35**, 91 (1984).
[10] J. V. Vukanić, R. K. Janev, and D. Heifetz, Nucl. Instrum. Methods B **18**, 131 (1987).
[11] R. Weissmann and P. Sigmund, Radiat. Eff. **19**, 7 (1973).
[12] J. Bøttiger and K. B. Winterbon, Radiat. Eff. **20**, 65 (1973).
[13] U. Littmark and A. Gras-Marti, Appl. Phys. **16**, 247 (1978).
[14] J. Bøttiger, J. A. Davies, P. Sigmund, and K. B. Winterbon, Radiat. Eff. **11**, 69 (1971).
[15] H. A. Bethe, M. E. Rose, and L. P. Smith, Proc. Am. Philos. Soc. **78**, 573 (1938).
[16] R. E. Marshak, Rev. Mod. Phys. **19**, 185 (1947).
[17] H. M. Urbassek and M. Vicanek, Phys. Rev. B **37**, 7256 (1988).
[18] J. Lindhard, M. Scharff, and H. E. Schiøtt, Mat. Fys. Medd. Dan. Vid. Selsk. **33**, No. 14 (1963); J. Lindhard, V. Nielsen, and M. Scharff, *ibid* **36**, No. 10 (1968).
[19] F. Oberhettinger and L. Badii, *Tables of Laplace Transforms* (Springer, Berlin, 1973).
[20] *Handbook of Mathematical Functions,* edited by M. Abramowitz and I. A. Stegun (Natl. Bur. Stand., Washington, D. C., 1965).
[21] N. Bohr, Mat. Fys. Medd. Dan. Vid. Selsk. **18**, No. 8 (1948).
[22] W. D. Wilson, L. G. Haggmark, and J. P. Biersack, Phys. Rev. B **15**, 2458 (1977).
[23] J. Lindhard and M. Scharff, Phys. Rev. **124**, 128 (1961).
[24] M. Vicanek and H. M. Urbassek, Nucl. Instrum. Methods B **30**, 507 (1988).
[25] C. K. Chen, W. Eckstein, and B. M. U. Scherzer, Appl. Phys. A **31**, 37 (1983).
[26] B. Davison, *Neutron Transport Theory* (Oxford University Press, London, 1957).
[27] I. S. Tilinin, Phys. Chem. Mech. Surfaces **2**, 640 (1984); **2**, 999 (1984).
[28] T. Tabata, R. Ito, K. Morita, and H. Tawara, Nucl. Instrum. Methods B **9**, 113 (1985).